Supporting Information

Lie et al. 10.1073/pnas.1202316109

SI Materials and Methods

Animals and Antibodies. Male Sprague–Dawley rats or pups were purchased from Charles River Laboratories. The use of animals in this study was approved by the Rockefeller University Institutional Animal Care and Use Committee (protocol nos. 09016 and 12506). Antibodies used in this study are listed in Table S1.

Construction of WT and Mutant Focal Adhesion Kinase Mammalian Expression Vectors. The full-length coding sequence of WT rat focal adhesion kinase (FAK; accession no. NM_013081.1), including start and stop codons, was amplified from rat Sertoli cell cDNA by PCR using primers listed in Table S2, and it was cloned into the MluI/XbaI site of the pCI-neo Mammalian Expression Vector (Promega). Single mutation of FAK-Tyr^{407} or FAK-Tyr^{397} to either phenylalanine or glutamic acid was performed by three-step mutagenic PCR (1), using the WT construct as the template. Each desired mutation was introduced by the amplification of two overlapping portions of FAK using two primer pairs (a mutagenic primer paired with a flanking primer with the opposite orientation; Table S2). The two PCR products were then fused together by overlap extension (1), from which the full-length cDNA was amplified with primers listed in Table S2. Similarly, double mutation was produced by three-step mutagenic PCR using a mutant construct as the template. The cDNAs encoding FAK mutants Y407F, Y407E, Y397F, Y397E, and Y397E-Y407E were cloned into pCI-neo Mammalian Expression Vector. All sequences were verified by direct DNA sequencing at Genewiz to confirm the mutant cDNA constructs. For the transfection into Sertoli cells, plasmid DNA was prepared with a HiSpeed Plasmid Midi Kit (Qiagen). For the visualization of transfected cells during fluorescence staining, plasmid DNA was labeled with Cy3 using a *Label*IT Tracker Intracellular Nucleic Acid Localization Kit (Mirus).

Overexpression of WT and Mutant FAK in Sertoli Cell Cultures. Primary Sertoli cells were isolated from testes of 20-d-old male Sprague–Dawley rats as described (2). Sertoli cells were plated at the appropriate cell density for each experiment. For the preparation of cell lysates, Sertoli cells were plated at 0.4×10^6 cells/cm^2 on Matrigel (BD Biosciences)-coated 6-well culture plates; for fluorescence staining, cells were plated at 0.04×10^6 cells/cm^2 on Matrigel-coated 25-mm glass coverslips; and for transepithelial electrical resistance (TER) measurement, cells were plated at 1.0×10^6 cells/cm^2 on Matrigel-coated Millicell-HA 12-mm culture plate inserts (Millipore). The inserts were then placed in 24-well dishes with 0.5 mL of F12/DMEM each in the apical and basal compartments. Sertoli cells were cultured for 2 d to allow the assembly of a tight junction (TJ)–permeability barrier (2), and the presence of TJs, basal ectoplasmic specializations (ES), gap junctions, and desmosomes in these cultures was confirmed by EM as described (3, 4). Thereafter, Sertoli cells were transfected with plasmid DNA (~0.4 μg per 10^6 cells) for 18 h using 15 μL of Effectene Transfection Reagent (Qiagen) per microgram of DNA according to the manufacturer's instructions (5). Cells were harvested 2 d after transfection for fluorescence microscopy and 3 d after transfection for the preparation of lysates. TER was measured once or twice daily throughout the period of culture as described (3).

Immunofluorescence Staining, Filamentous Actin Staining. Frozen sections (7 μm) of adult rat testes obtained in a cryostat at −22°C or Sertoli cells were fixed in 4% (wt/vol) paraformaldehyde in PBS for 10 min. For immunofluorescence and filamentous (F)-actin staining, sections or cells were permeabilized in 0.1% (vol/vol) Triton X-100 in PBS (10 mM sodium phosphate, 0.15M NaCl, pH 7.4 at 22°C) and blocked with 1% (wt/vol) BSA in PBS for 30 min. This was followed by an overnight incubation of primary antibodies listed in Table S1 (1:100–200 in 1% BSA) and then a 30-min incubation of Alexa Fluor-conjugated secondary antibodies (Invitrogen; 1:250 for sections and 1:100 for cells in 1% BSA). For F-actin staining, sections or cells were incubated with FITC-conjugated phalloidin (Sigma–Aldrich; 1:70 in 1% BSA) for 30 min, either alone or together with a secondary antibody in dual-labeled immunofluorescence staining. Sections or cells were mounted in ProLong Gold antifade reagent with 4′,6-diamidino-2-phenylindole (DAPI) (Invitrogen). All incubations were performed at room temperature. Images were acquired with an Olympus BX61 fluorescence microscope (Olympus Imaging America) equipped with an Olympus DP70 12.5MPx digital camera and MicroSuite FIVE software package (Version 1224) (Olympus Soft Imaging Solutions Corp.). All images in TIFF format were analyzed in Adobe PhotoShop, such as image overlays, using the Adobe Creative Suite (version 3.0). In experiments wherein the effects of overexpression of different FAK mutants versus the corresponding control on the localization and/or distribution of proteins (or F-actin organization) at the Sertoli cell BTB were examined, different samples within the experimental and the control groups were processed simultaneously in a single experimental session to avoid interexperimental variations. All imaging data presented here were the results of a representative experiment. However, each experiment was repeated at least 3–4 times in independent experiments using different batches of Sertoli cells and yielded similar results.

Confocal Microscopy. Confocal microscopy was performed at The Rockefeller University Bio-Imaging Resource Center as previously described (6, 7). In short, Sertoli cells were cultured at 0.75×10^6 cells/cm^2 for 3 d on Matrigel-coated Costar polyester membrane inserts (24-mm diameter, 0.4-μm pore size; Corning), with each insert placed in a six-well dish to allow the establishment of a functional TJ–permeability barrier. Cells were then transfected with pCI-neo and different FAK constructs for 24 h. Two days thereafter, cultures on polyester membranes were terminated using a fixative of 4% (wt/vol) paraformaldehyde in PBS (10 min), permeabilized in 0.1% (vol/vol) Triton X-100/PBS (4 min), and blocked with 1% (wt/vol) BSA/PBS (30 min). Sertoli cells were stained with anti–actin-related protein (Arp) 3 or an anti–claudin-11 antibody (Table S1) at room temperature (22 °C) overnight, followed by incubation with Alexa Fluor 488-conjugated goat anti-mouse (for Arp3) or goat anti-rabbit (for claudin-11) secondary antibody (Invitrogen) at a 1:100 dilution in PBS containing 1% (wt/vol) BSA at 22 °C for 30 min. Images were obtained using an inverted Zeiss LSM510 laser scanning confocal microscope (Carl Zeiss MicroImaging) with three single-photon lasers (Ar, HeNe 543, and HeNe 633) and Zeiss LSM 510 software (Carl Zeiss MicroImaging). Optical sections of ~0.8 μm were collected at 0.25-μm intervals along the *z* axis to obtain a series of images (i.e., Z stack). Image deconvolution of Z stacks was performed using 3D Huygens Deconvolution Software (Scientific Volume Imaging) to increase the signal-to-noise ratio. *Z* stacks were adjusted for brightness and contrast,

and optical sections were reconstructed with ImageJ software (version 1.45; US National Institutes of Health).

Actin Polymerization Assay. Lysates of transfected Sertoli cells were prepared in Tris lysis buffer [20 mM Tris (pH 7.5) at 22 °C, containing 20 mM NaCl and 0.5% (vol/vol) Triton X-100, freshly supplemented with Protease Inhibitor Mixture (Sigma–Aldrich) for use with mammalian cell and tissue extracts and Phosphatase Inhibitor Mixtures 2 and 3 (Sigma–Aldrich), each at 1:66.7 dilution]. Lysates were homogenized with syringe needles, cleared by centrifugation at 20,817 × *g* for 2.5 h at 4 °C, and diluted to the same protein concentration (~8.5 mg/mL). The effect of these lysates on actin polymerization in vitro was immediately assayed with an Actin Polymerization Biochem Kit (Cytoskeleton, Inc.) according to the manufacturer's instruction. Each reaction mixture consisted of the following at a ratio of 6:3:1: (*i*) pyrene-labeled muscle actin [0.5 mg/mL in 5 mM Tris·HCl (pH 8.0) containing 0.2 mM $CaCl_2$ and freshly supplemented with 0.2 mM ATP], (*ii*) Sertoli cell lysate prepared as described above, and (*iii*) actin polymerization buffer [100 mM Tris·HCl (pH 7.5) containing 500 mM KCl, 20 mM $MgCl_2$, and 10 mM ATP]. The polymerization of pyrene-labeled actin was reflected by the increase in fluorescence emission at 395–440 nm, which was measured in a black 96-well plate (via top reading) with a FilterMax F5 Multi-Mode Microplate Reader (Molecular Devices). A kinetic reading was taken at room temperature every 20 s for 100 cycles (excitation wavelength = 360 nm, emission wavelength = 430 nm, integration time = 0.25 ms) using a Multi-Mode Analysis Software package (version 3.4; Molecular Devices). The rate of increase in fluorescence intensity during the initial linear phase of the reaction (first 3–5 min) was estimated by linear regression using Microsoft Excel.

General Methods. Germ cells and seminiferous tubules were isolated as described (3). For coimmunoprecipitation and immunoblotting, cell and tissue lysates were prepared in IP (immunoprecipitation) lysis buffer [50 mM Tris (pH 7.4) at 22 °C containing 150 mM NaCl, 2 mM EGTA, 10% (vol/vol) glycerol, and 1% (vol/vol) Nonidet P-40 and freshly supplemented with Protease Inhibitor Mixture for use with mammalian cell and tissue extracts (1:100; Sigma–Aldrich) and Phosphatase Inhibitor Mixtures 2 and 3 (1:80; Sigma–Aldrich)]. For coimmunoprecipitation, lysates containing 300–500 μg of protein were precleared with normal rabbit or mouse IgG (3 μg of antibody for each milligram of lysate protein) for 2 h. Protein complexes were pulled down by incubation with Protein A/G PLUS Agarose (Santa Cruz) for 2 h, and the beads were discarded; the cleared lysates were then incubated overnight with specific antibodies (4 μg of antibody for each milligram of lysate protein). Protein complexes were immunoprecipitated with Protein A/G PLUS Agarose for 4–5 h. All incubations were performed at room temperature in a laboratory rotator. Beads were washed, proteins were resolved by SDS/PAGE, and interacting proteins were identified by immunoblotting using corresponding antibodies as described (3, 8).

Statistical Analysis. GB-STAT 7.0 software (Dynamic Microsystems, Inc.) was used for statistical analysis. The Student *t* test (two-tailed) was used for paired comparisons. One-way ANOVA was used for the comparison of three or more groups, which was followed by either Dunnett's test against the control or the Newman–Keuls test for comparisons among all groups (only selected comparisons were shown).

SI Discussion

It remains to be fully understood exactly how Arp2/3 activity influences cell junction integrity in the seminiferous epithelium. A previous study from our laboratory has linked Arp2/3 activity to junction-restructuring events at the degenerating apical ES at the concave side of elongating spermatid heads, as well as the blood–testis barrier (BTB), which must "open and/or restructure" transiently from stage VIII to stage XI to allow the transit of preleptotene spermatocytes (8). The Arp2/3 complex is well known to nucleate the highly branched actin network characteristic of lamellipodia, generating the necessary force to propel the leading edge of migrating cells (9, 10). Although Sertoli cells do not migrate, per se, in vivo, it is conceivable that lamellipodia-like structures could support minor movements needed for the dynamic restructuring at the cell-cell interface. In this study, however, Arp2/3 activity is correlated with cell junction stabilization instead of restructuring. This can be explained for the following reasons. First, the Arp2/3 complex is only one of the many effectors of p-FAK-Tyr^{407}, which is also illustrated by the fact the p-FAK-Tyr^{407} is constantly found at the BTB but Arp3 is only transiently recruited at stage VIII of the epithelial cycle (8). Thus, the observed tightening of the tight junction (TJ) barrier after FAK Y407E phosphomimetic mutation may be attributed to additional effectors other than the Arp2/3 complex. Second, despite the fact that Arp2/3 activity generally results in a highly branched actin network, emerging evidence suggests that Arp2/3-mediated actin nucleation is also involved in the assembly of transverse arcs, a subset of actin stress fibers that are not directly anchored to the substrate (11). This may explain why the Arp2/3 complex supports restructuring events in the seminiferous epithelium (8) but could also be required for the assembly of robust actin filament bundles underneath the plasma membrane to stabilize cell junctions as reported herein.

The mechanistic details of how FAK-Tyr^{407} phosphorylation leads to increased neuronal Wiskott–Aldrich syndrome protein (N-WASP)/Arp3 association and enhanced Arp2/3 activity are not presently addressed. It is known that Arp3 directly binds the 4.1/ezrin/radixin/moesin domain of FAK, and this association is destabilized when FAK-Tyr^{397} is phosphorylated (12). Although FAK/Arp3 interaction could not be detected in our coimmunoprecipitation experiment, this could be attributable to the limitations of the antibody used, and we cannot rule out the possibility that FAK might actually bind Arp3 in the seminiferous epithelium. If that is the case, Tyr^{407} phosphorylation could serve to suppress Tyr^{397} phosphorylation, leading to a stabilization of the protein complex constituted by FAK, the Arp2/3 complex, and N-WASP, thereby promoting Arp2/3 activity. An outstanding question is whether a modulation in the kinase activity of FAK or the FAK/Src complex is required for Arp2/3 activation following Tyr^{407} phosphorylation. Because N-WASP was reported to be a substrate of FAK (13), it is of interest to determine how FAK-Tyr^{407} phosphorylation affects the phosphorylation status of N-WASP, and how this, in turn, contributes to the final phenotype.

1. Vallejo AN, Pogulis RJ, Pease LR (2008) PCR mutagenesis by overlap extension and gene SOE. *CSH Protoc*, 10.1101/pdb.prot4861.
2. Mruk DD, Cheng CY (2011) An *in vitro* system to study Sertoli cell blood-testis barrier dynamics. *Methods Mol Biol* 763:237–252.
3. Lie PPY, Cheng CY, Mruk DD (2010) Crosstalk between desmoglein-2/desmocollin-2/Src kinase and coxsackie and adenovirus receptor/ZO-1 protein complexes, regulates blood-testis barrier dynamics. *Int J Biochem Cell Biol* 42:975–986.
4. Siu MKY, Wong CH, Lee WM, Cheng CY (2005) Sertoli-germ cell anchoring junction dynamics in the testis are regulated by an interplay of lipid and protein kinases. *J Biol Chem* 280:25029–25047.
5. Yan HHN, Mruk DD, Wong EWP, Lee WM, Cheng CY (2008) An autocrine axis in the testis that coordinates spermiation and blood-testis barrier restructuring during spermatogenesis. *Proc Natl Acad Sci USA* 105:8950–8955.
6. Lie PPY, Cheng CY, Mruk DD (2011) Interleukin-1α is a regulator of the blood-testis barrier. *FASEB J* 25:1244–1253.

7. Su L, Mruk DD, Lui WY, Lee WM, Cheng CY (2011) P-glycoprotein regulates blood-testis barrier dynamics via its effects on the occludin/zonula occludens 1 (ZO-1) protein complex mediated by focal adhesion kinase (FAK). *Proc Natl Acad Sci USA* 108:19623–19628.
8. Lie PPY, Chan AYN, Mruk DD, Lee WM, Cheng CY (2010) Restricted Arp3 expression in the testis prevents blood-testis barrier disruption during junction restructuring at spermatogenesis. *Proc Natl Acad Sci USA* 107:11411–11416.
9. Goley ED, Welch MD (2006) The ARP2/3 complex: An actin nucleator comes of age. *Nat Rev Mol Cell Biol* 7:713–726.
10. Weaver AM, Young ME, Lee WL, Cooper JA (2003) Integration of signals to the Arp2/3 complex. *Curr Opin Cell Biol* 15:23–30.
11. Hotulainen P, Lappalainen P (2006) Stress fibers are generated by two distinct actin assembly mechanisms in motile cells. *J Cell Biol* 173:383–394.
12. Serrels B, et al. (2007) Focal adhesion kinase controls actin assembly via a FERM-mediated interaction with the Arp2/3 complex. *Nat Cell Biol* 9:1046–1056.
13. Wu X, Suetsugu S, Cooper LA, Takenawa T, Guan JL (2004) Focal adhesion kinase regulation of N-WASP subcellular localization and function. *J Biol Chem* 279:9565–9576.

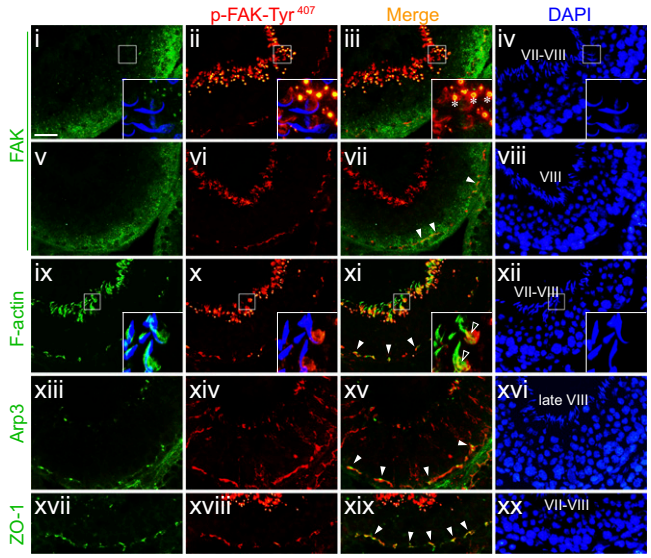

Fig. S1. Colocalization of p-FAK-Tyr^{407} with BTB and apical ES proteins and F-actin in the seminiferous epithelium of adult rat testes. Dual-labeled immunofluorescence staining of FAK (*i* and *v*; green), F-actin (*ix*; green), Arp3 (*xiii*; green), or zonula occludens (ZO)-1 (*xvii;* green) with p-FAK-Tyr^{407} (red) in frozen sections of adult rat testes. Colocalization of FAK, F-actin, Arp3, or ZO-1 with p-FAK-Tyr^{407} are shown in *i–viii*, *ix–xii*, *xiii–xvi*, and *xvii–xx*, respectively. Nuclei were visualized with DAPI. Stages of the tubules are annotated by roman numerals. (*Insets*) Boxed areas in selected micrographs are magnified. At the BTB, p-FAK-Tyr^{407} was found to colocalize with FAK, F-actin, Arp3, and ZO-1 (white arrowheads in *vii*, *xi*, *xv*, and *xix*). In addition, p-FAK-Tyr^{407} was found to colocalize with FAK in vesicle-like structures (asterisks in *Inset* in *iii)* near the tubule lumen and with F-actin at the concave side of elongated spermatid heads (open arrowheads in *Inset* in *xi*). (Scale bar: 40 μm.)

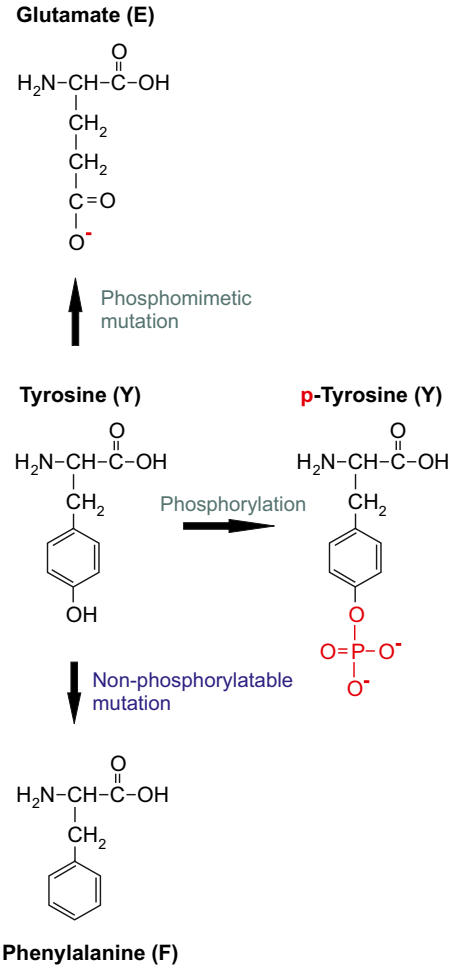

Fig. S2. Nonphosphorylatable and phosphomimetic mutations on tyrosine of p-FAK-Tyr^{407} or p-FAK-Tyr^{397}. By replacing tyrosine (Tyr, Y) with phenylalanine (Phe, F), the lack of an OH^- group renders the mutant nonphosphorylatable, whereas glutamate (Glu, E) serves as a phosphorylation mimicking mutant by introducing a negative charge. cDNAs encoding these mutants are prepared by site-directed mutagenesis essentially as previously described (1) and detailed in *SI Materials and Methods*, and they were cloned into pCI-neo Mammalian Expression Vector. Mutations were confirmed by direct DNA sequencing.

1. Mruk DD, Wong CH, Silvestrini B, Cheng CY (2006) A male contraceptive targeting germ cell adhesion. *Nat Med* 12:1323–1328.

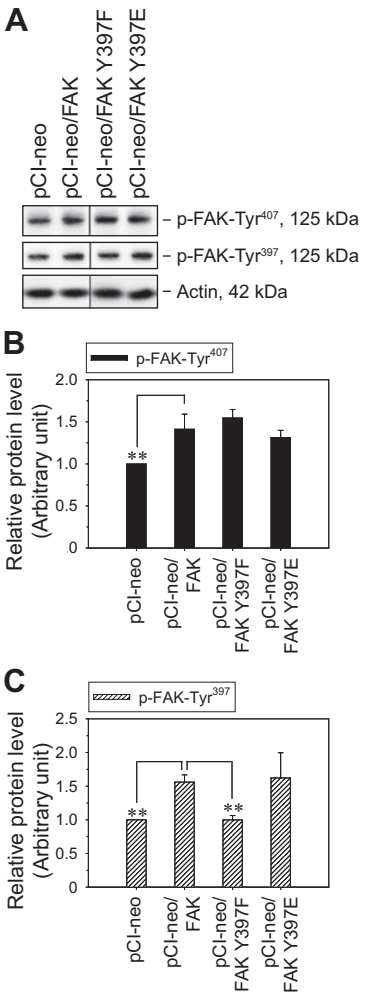

Fig. S3. Effect of FAK-Tyr^{397} mutations on the phosphorylation status of FAK-Tyr^{407}. (*A*) Immunoblot analysis of p-FAK-Tyr^{407} and p-FAK-Tyr^{397} in Sertoli cells following the transfection of pCI-neo vector, WT FAK, nonphosphorylatablde mutant FAK Y397F, and phosphomimetic mutant FAK Y397E. Sertoli cells (0.4×10^6 cells/cm^2) cultured for 2 d with an established functional TJ–permeability barrier were transfected with plasmid DNA. Lysates harvested 3 d thereafter were subjected to immunoblotting, with 25 μg of proteins loaded in each lane. Actin serves as a control for subsequent quantification analysis. (*B* and *C*) Histograms summarize immunoblotting results as in *A* from several independent experiments. Each data point was normalized against the corresponding actin level and then against the protein level in pCI-neo, which was arbitrarily set as 1. Each bar is a mean ± SD of $n = 3–6$. $^{**}P < 0.01$ vs. pCI-neo/FAK; one-way ANOVA followed by the Newman–Keuls test.

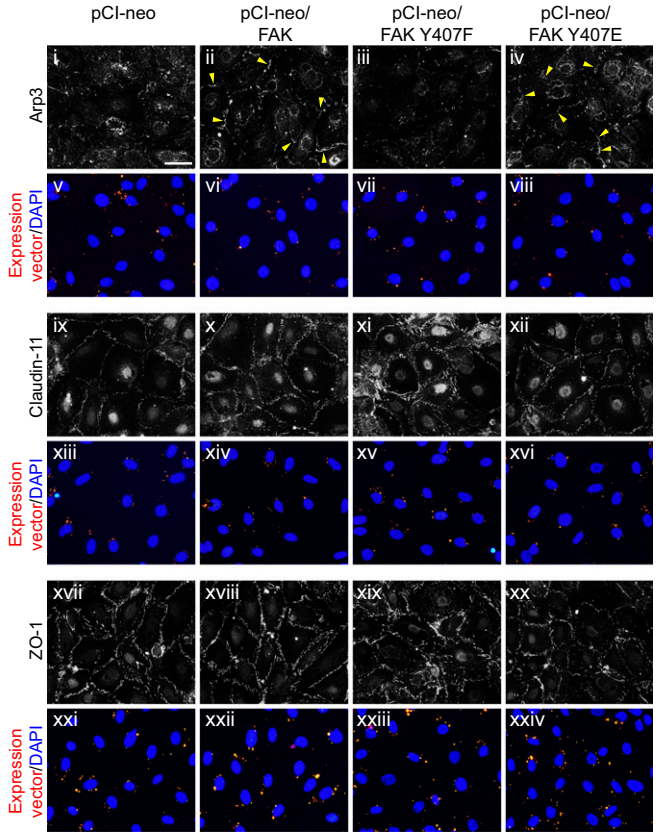

Fig. S4. Low-magnification micrographs show the effects of FAK-Tyr^{407} mutations on the localization of Arp3 and BTB constituent proteins in Sertoli cells in vitro. Sertoli cells (0.04×10^6 cells/cm^2) cultured for 2 d were transfected with Cy3-labeled plasmid DNA of pCI-neo vector only vs. WT FAK and FAK mutants. Two days thereafter, cells were fixed and processed for immunofluorescence staining of Arp3 (*i–iv*), claudin-11 (*ix–xii*), or zonula occludens (ZO)-1 (*xvii–xx*). Immunofluorescence staining is shown in gray scale to better visualize the localization of corresponding proteins at the Sertoli cell-cell interface following transfection. Corresponding images of cell nuclei stained with DAPI (blue), and Cy3-labeled expression constructs (red) are shown in *v–viii*, *xiii–xvi*, *and xxi–xiv* to illustrate successful transfection. Overexpression of both WT FAK and phosphomimetic mutant FAK Y407E caused up-regulation of Arp3 at the cell-cell interface (yellow arrowheads in *ii and iv*), whereas overexpression of FAK Y407F caused mislocalization of TJ proteins claudin-11 (*xi*) and ZO-1 (*xix*), moving away from the cell-cell interface into the Sertoli cell cytosol, showing signs of protein internalization. (Scale bar: 50 μm.) Changes in the localization of Arp3 and claudin-11 were further verified by confocal microscopy (Fig. S5).

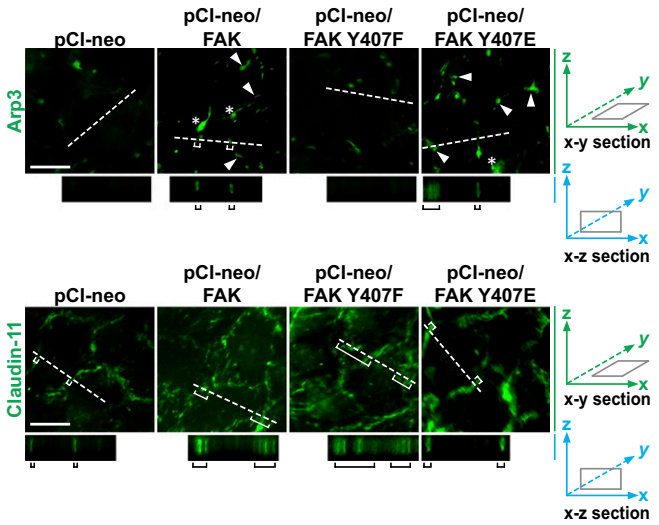

Fig. S5. Study by confocal microscopy to assess the effects of FAK-Tyr^{407} mutations on the localization of Arp3 and claudin-11 at the Sertoli cell BTB in vitro. To validate the results shown in Fig. 5 on changes in the localization of BTB constituent proteins at the Sertoli cell-cell interface following expression of FAK constructs, confocal microscopy was used. Sertoli cells (0.75×10^6 cells/cm^2) cultured alone for 2 d were transfected with pCI-neo vector alone vs. WT FAK and FAK mutants. Two days after transfection, Z stacks of the Sertoli cell epithelium stained for Arp3 (green fluorescence) or claudin-11 (green fluorescence) were obtained. (*Upper*) Each column shows an optical slice from the *x-y* plane (i.e., parallel to the plane of cell attachment shown in the green *x-y* section). (*Lower*) Micrographs are vertical views of the Sertoli cell epithelium, which are reconstructed optical slices from the *x-z* plane (i.e., perpendicular to the plane of cell attachment, blue *x-z* section) corresponding to the sliced positions in the *x-y* plane marked by white dotted lines and white brackets. Brackets in white (*Upper*) correspond to brackets in black (*Lower*) for either Arp3 or claudin-11. For Arp3, expression of the pCI-neo/FAK and phosphomimetic mutant pCI-neo/FAK Y407E but not of nonphosphorylatable mutant pCI-neo/FAK Y407F or pCI-neo alone was found to induce the aggregation of Arp3 at the Sertoli cell-cell interface (white arrowheads), producing very intense signals (annotated by an asterisk). For claudin-11, expression of nonphosphorylatable mutant FAK Y407F (pCI-neo/FAK Y407F) led to its internalization, moving away from the cell-cell interface, as shown by diffused signals in the *x-z* view. In short, these additional analyses confirmed results shown in Fig. 5 regarding changes in the localization of these proteins following expression of the FAK Y407E mutant. These findings are representative results of three independent experiments. (Scale bar: 15 μm.)

Table S1. Antibodies used in this study

Antibody	Vendor	Catalog no.	Application and dilution
Goat antiactin	Santa Cruz Biotechnology	sc-1616	IB (1:300)
Mouse anti-Arp3	Sigma–Aldrich	A5979	IB (1:3,000), IF (1:200)
Rabbit anti–N-cadherin	Santa Cruz Biotechnology	sc-7939	IB (1:200)
Rabbit anti–β-catenin	Invitrogen	71-2700	IB (1:125)
Rabbit anti–claudin-11	Invitrogen	36-4500	IB (1:125), IF (1:100)
Mouse anti-Eps8	BD Biosciences	610143	IB (1:5,000), IF (1;100)
Rabbit anti-FAK	Santa Cruz Biotechnology	sc-558	IB (1:200)
Mouse anti-FAK	Millipore	05-537	IF (1:100)
Rabbit anti–p-FAK-Tyr^{397}	Invitrogen	44625G	IB (1:1,000)
Rabbit anti–p-FAK-Tyr^{397}	Thermo Fisher Scientific	PAI-22001	IF (1:100)
Rabbit anti–p-FAK-Tyr^{407}	Invitrogen	44650G	IB (1:1,000), IF (1:100)
Rabbit anti–β1-integrin	Millipore	AB1952	IF (1:100)
Rabbit anti-occludin	Invitrogen	71-1500	IB (1:125)
Mouse anti–c-Src	Santa Cruz Biotechnology	sc-8056	IB (1:200)
Rabbit anti–p-Src-Tyr^{418}	Millipore	07-909	IB (1:1,000)
Rabbit anti–N-WASP	Santa Cruz Biotechnology	sc-20770	IB (1:200), IP (1:25)
Rabbit anti–ZO-1	Invitrogen	61-7300	IB (1:125), IF (1:100)

IB, immunoblotting; IF, immunofluorescence microscopy; IP, immunoprecipitation; ZO, zonula occludens. Antibodies used for experiments reported herein cross-reacted with the corresponding proteins in the rat as indicated by the manufacturers.

Table S2. Primers used for the construction of different FAK expression vectors

Target sequence/mutation	Accession no.	Primer orientation	Primer sequence (5′→3′)	Nucleotide position
Primers for the amplification of full-length rat FAK				
FAK	NM_031081.1	S	GTACGCGTCTAGCAAAAGAATGGCAGCTGCT	421–443
		AS	AGTCTAGATCAGTGTGGCCGTGTCTGCCCT	3,578–3,599
Mutagenic primers used during three-step mutagenic PCR of FAK				
FAK Tyr^{407}→Phe	NM_031081.1	S	CATCGATGAGGAAGACACATTTACCATGCCCTCAACCAGGG	1,631–1,671
		AS	CCCTGGTTGAGGGCATGGTAAATGTGTCTTCCTCATCGATG	1,631–1,671
FAK Tyr^{407}→Glu	NM_031081.1	S	CATCGATGAGGAAGACACAGAAACCATGCCCTCAACCAGGG	1,631–1,671
		AS	CCCTGGTTGAGGGCATGGTTTCTGTGTCTTCCTCATCGATG	1,631–1,671
FAK Tyr^{397}→Phe	NM_031081.1	S	TGTGTCAGAGACAGATGACTTTGCCGAGATCATCGATGAGG	1,601–1,641
		AS	CCTCATCGATGATCTCGGCAAAGTCATCTGTCTCTGACACA	1,601–1,641
FAK Tyr^{397}→Glu	NM_031081.1	S	TGTGTCAGAGACAGATGACGAAGCCGAGATCATCGATGAGG	1,601–1,641
		AS	CCTCATCGATGATCTCGGCTTCGTCATCTGTCTCTGACACA	1,601–1,641
Flanking primers used during three-step mutagenic PCR of FAK				
pCI-neo	U47120.2	S	GGCTAGAGTACTTAATACGACTC	1,055–1,077
FAK	NM_031081.1	AS	AGTCTAGATCAGTGTGGCCGTGTCTGCCCT	3,578–3,599

Sequences marked by dotted underlining represent the restriction enzyme recognition sites added for cloning into pCI-neo Mammalian Expression Vector. Sequences marked by solid underlining represent sites of mutation on FAK. S, sense; AS, antisense.